BIOMOLECULES & THERAPEUTICS

Original Article
Biomol Ther 28(1), 92-97 (2020)

Lodoxamide Attenuates Hepatic Fibrosis in Mice: Involvement of GPR35

Mi-Jeong Kim, Soo-Jin Park, So-Yeon Nam and Dong-Soon Im*

College of Pharmacy, Pusan National University, Busan 46241, Republic of Korea

Abstract

A previous pharmacogenomic analysis identified cromolyn, an anti-allergic drug, as an effective anti-fibrotic agent that acts on hepatocytes and stellate cells. Furthermore, cromolyn was shown to be a G protein-coupled receptor 35 (GPR35) agonist. However, it has not been studied whether anti-fibrotic effects are mediated by GPR35. Therefore, in this study, the role of GPR35 in hepatic fibrosis was investigated through the use of lodoxamide, another anti-allergic drug and a potent GPR35 agonist. Long-term treatment with carbon tetrachloride induced hepatic fibrosis, which was inhibited by treatment with lodoxamide. Furthermore, CID2745687, a specific GPR35 antagonist, reversed lodoxamide-mediated anti-fibrotic effects. In addition, lodoxamide treatment showed significant effects on the mRNA expression of collagen Iα1, collagen Iα2, and TGF-β1 in the extracellular matrix. However, a transforming growth factor α (TGF-α) shedding assay revealed lodoxamide not to be a potent agonist of mouse GPR35 *in vitro*. Therefore, these results showed anti-fibrotic effects of lodoxamide in mice and raise concerns how lodoxamide protects against liver fibrosis *in vivo* and whether GPR35 is involved in the action.

Key Words: Fibrosis, Liver, Lodoxamide, CID2745687, Carbon tetrachloride

INTRODUCTION

Liver fibrosis results from acute damage and the subsequent wound-healing response to injury and may eventually cause liver cirrhosis and liver failure (Bataller and Brenner, 2005). Hepatic stellate cells have been studied for the development of anti-fibrotic chemicals, and epithelial-mesenchymal transition of hepatocytes has become accepted as a mechanism for the development of hepatic fibrosis (Choi *et al*., 2015). Recently, a pharmacogenomic study identified cromolyn, a mast cell stabilizer, as an anti-fibrotic agent targeting both hepatocytes and hepatic stellate cells (Choi *et al*., 2015). Moreover, cromolyn was identified as a G protein-coupled receptor 35 (GPR35) agonist (Yang *et al*., 2010).

Human GPR35 is an orphan G protein-coupled receptor that is expressed in immune cells and in the colon, lungs, small intestine, spleen, and stomach in humans (O'Dowd *et al*., 1998; Wang *et al*., 2006; Fallarini *et al*., 2010; Yang *et al*., 2010). In a previous study, we demonstrated the expression of GPR35 in human and mouse hepatocytes (Nam *et al*., 2019). Many synthetic surrogate agonists and antagonists have been developed or identified (Taniguchi *et al*., 2006; Heynen-Genel *et al*., 2010a, 2010b; Jenkins *et al*., 2010; Zhao *et al*., 2010; Jenkins *et al*., 2012; Funke *et al*., 2013; Neetoo-Isseljee *et al*., 2013; Thimm *et al*., 2013; MacKenzie *et al*., 2014). Although cromolyn is reported to act as an anti-fibrotic agent in hepatic fibrosis and as a GPR35 agonist, the role of GPR35 in hepatic fibrosis has not yet been studied. Lodoxamide is another anti-allergic drug and a potent agonist of human and rodent GPR35 (MacKenzie *et al*., 2014). Therefore, the function of GPR35 in hepatic fibrosis was investigated in a carbon tetrachloride (CCl_4)-induced hepatic fibrosis model, by using lodoxamide, a potent GPR35 agonist, and CID2745687, a selective GPR35 antagonist (MacKenzie *et al*., 2014; Park *et al*., 2018).

MATERIALS AND METHODS

Materials

Lodoxamide (L469365, molecular weight=311.63 g/mol, PubChem ID 44564) was purchased from Toronto Research Chemicals Inc. (North York, ON, Canada), and CID2745687 (4293, ≥98% purity as determined via high-performance liquid chromatography (HPLC), molecular weight=395.43 g/mol,

Open Access **https://doi.org/10.4062/biomolther.2018.227**

Received Nov 26, 2018 **Revised** May 7, 2019 **Accepted** May 21, 2019
Published Online Jun 13, 2019

***Corresponding Author**
E-mail: imds@pusan.ac.kr
Tel: +82-51-510-2817, Fax: +82-51-513-6754

PubChem ID 9581011) from Tocris (Ellisville, MO, USA). Plasmids for alkaline phosphatase (AP)-tagged TGF-α shedding assay (an AP fusion protein of TGF-α, human GPR35, and eight Gα proteins) were kindly provided by Dr. Junken Aoki at Tohoku University. A mouse GPR35 plasmid (NP_071715) was purchased from R&D system (Minneapolis, MN, USA). Others were obtained from Sigma-Aldrich (St. Louis, MO, USA).

Animals

C57BL/6 mice were housed in a Laboratory Animal facility in Pusan National University (PNU), and provided with food and water *ad libitum*. The animal protocol used in this study was reviewed and approved by the PNU–Institutional Animal Care Committee (PNU–IACUC) with respect to procedure ethics and scientific care (Approval Number PNU-2018-2049).

Induction of hepatic fibrosis in C57BL/6 mice

Six-week-old male C57BL/6 mice were purchased from Daehan Biolink (DBL, Seoul, Korea) and housed under standard laboratory conditions (22°C ± 2°C, 12-h light/dark cycles) with free access to food and water in the laboratory animal facility at PNU. In this study, seven-week-old male C57BL/6 mice were randomly divided into 4 groups : control (n=5), in which mice were intraperitoneal (i.p.) injected a vehicle for 8 weeks; CCl_4 (n=5), in which mice were i.p. injected a CCl_4 (5 ml/kg, CCl_4:con oil=2:8) twice a week for 8 weeks; CCl_4 plus lodoxamide (n=5), in which mice were i.p. injected a CCl_4 two times a week for 8 weeks and oral administration with lodoxamide (1 mg/kg) every day of the last 4 weeks; and CCl_4 plus lodoxamide and CID2745687 (n=5), in which mice were i.p. injected a CCl_4 two times a week for 8 weeks, and oral administration of lodoxamide (1 mg/kg) and CID2745687 (1 mg/kg) every day of the last 4 weeks.

Measurement of aspartate aminotransferase (AST or GOT) and alanine aminotransferase (ALT or GPT)

Serum AST (GOT) and ALT (GPT) levels were measured by using kits (AM103-K and AM102-K) from Asan Pharmaceutical (Seoul, Korea).

Histological analysis of the liver

After sacrificing the mice, liver tissues were fixed in 10% formalin and dehydrated in 30% sucrose solution in phosphate buffered saline (PBS, pH 7.4) overnight at 4°C and embedded in optimal cutting temperature (OCT) compound. Sections (8 μm) were then thaw-mounted onto microslides (Muto pure chemicals Co., Ltd, Tokyo, Japan) and stored at –80°C until further use. Sections were stained with hematoxylin and eosin (H&E) or Masson's trichrome stain. For H&E staining, sections were removed OCT compound in distilled water for 5 min, hydrated, counterstained with hematoxylin solution (S3309, Dako, Glistrup, Denmark) for 15 s, washed in warm running tap water, and stained with eosin reagent for 10 s. The sections were then rinsed, dehydrated, and mounted onto slides using Permount medium, and covered with coverslips. To confirm collagen production via Masson's trichrome staining, sections were removed OCT compound in distilled water for 5 min, stained in Bouin's solution for 1 min using microwave, and allowed to stand for 15 min at room temperature. After washing in running tap water for 5 min, sections were placed in hematoxylin (H9627, Sigma-Aldrich) for 10 min, rinsed with running tap water for 10 min, stained in Biebrich scarlet (HT151, Sigma-Aldrich) for 5 min, and washed with distilled water three times. Thereafter, sections were stained with phosphotungstic/phosphomolybdic acid for 5 min and transferred directly to aniline blue for 10 min. The sections were then rinsed with distilled water three times, dehydrated and covered with coverslips.

Liver injury and fibrosis were scored by a treatment-blind observer. Degree of liver injury was scored using a subjective scale of 0-5 in H&E stained tissue. In brief, a score of 0 indicated no liver injury, 1 indicated <10% liver injury, 2 indicated 10-25% liver injury, 3 indicated 25-50% liver injury, 4 indicated 50-70% liver injury, 5 indicated >75% liver injury depending on the percentage of damaged area (Lim *et al*., 2016). Degree of liver fibrosis was evaluated using Ishak stage of 0-5 in Masson's trichrome stained tissue. In brief, a stage of 0 indicated no fibrosis (normal), 1 indicated fibrosis expansion of some portal areas with or without short fibrous septa, 2 indicated fibrosis expansion of most portal areas with or without short fibrous septa, 3 indicated fibrosis expansion of most portal areas with occasional portal to portal bridging, 4 indicated fibrosis expansion of portal areas with marked portal to portal bridging and/or portal to central bridging, 5 indicated cirrhosis (Lim *et al*., 2016; Nallagangula *et al*., 2017).

Reverse transcriptase polymerase chain reaction (RT-PCR)

To assess the expression of fibrotic markers via RT-PCR, first-strand complementary DNA (cDNA) was synthesized from total RNA isolated from liver tissues using Trizol reagent (Invitrogen, Waltham, MA, USA). Synthesized cDNA products, primers for each gene, and Promega Go-Taq® DNA polymerase (Promega Corporation, Madison, WI, USA) were used for PCR. Specific primers for collagen Iα1 (sense 5'-CAC CCT CAA GAG CCT GAG TC-3', antisense 5'-GTT CGG GCT GAT GTA CCA GT-3', 253 base pairs (bp)), collagen IIIα1 (sense 5'-GTC CAC GAG GTG ACA AAA GT-3', antisense 5'-GAT GCC CAC TTG TTC CAT CT-3', 204 bp) were used to amplify gene fragments. PCR was performed 32 amplification cycles of denaturation at 95°C for 30 s, annealing at 55°C for 30 s, and elongation at 72°C for 30 s using a SimpliAmp Thermal Cycler PCR machine (Thermo Fisher Scientific, Waltham, MA, USA). Specific primers for collagen Iα2 (sense 5'-TGG CCC ATC TGG TAA AGA AG-3', antisense 5'-ACC TTT GCC ACC TTG AAC AC-3', 256 bp) was used and annealing was performed at 53°C (34 amplication cycles). Specific primers for, α smooth muscle actin (αSMA, sense 5'-CTG ACA GAG GCA CCA CTG AA-3', antisense 5'-GAA GGA ATA GCC ACG CTC AG-3', 288 bp) was used and annealing was performed at 54°C (31 amplication cycles). Specific primers for TIMP metallopeptidase inhibitor 1 (TIMP1, sense 5'-TCC CCA GAA ATC AAC GAG AC-3', antisense 5'-CTC AGA GTA CGC CAG GGA AC-3', 251 bp) was used and annealing was performed at 52°C (30 amplication cycles). Specific primers for transforming growth factor β 1 (TGF-β1, sense 5'-GCC CTG GAT ACC AAC TAT TG-3', antisense 5'-AGC TGC ACT TGC AGG AGC G-3', 340 bp) was used and annealing was performed at 55°C (30 amplication cycles). Specific primers for fibronectin (sense 5'-ACC ACC CAG AAC TAC GAT GC-3', antisense 5'-GGA ACG TGT CGT TCA CAT TG-3', 253 bp) was used and annealing was performed 53°C (28 amplication cycles). Specific primers for glyceraldehyde 3-phopshate dehydrogenase (GAPDH, sense 5'-TTC ACC ACC ATG GAG

AAG GC-3', antisense 5'-GGC ATG GAC TGT GGT CAT GA-3', 237 bp) was used and annealing was performed at 60°C (27 amplication cycles) (Park and Im, 2019). Aliquots (7 μl) were subjected to electrophoresis on 1.2% agarose gels and stained with StaySafe™ Nucleic Acid Gel Stain (Real Biotech Corporation, Taipei, Taiwan).

AP-TGF-α shedding assay

HEK-293 cells (ATCC, Manassas, VA, USA) were cultured at 37°C in a 5% CO_2 humidified incubator and maintained in high-glucose Dulbecco's modified Eagle's medium (DMEM) containing 10% (v/v) heat-inactivated fetal bovine serum, 100 units/mL penicillin, 50 μg/mL streptomycin, 2 mM glutamine, and 1 mM sodium pyruvate.

HEK-293 cells were seeded at a density of 2.0×10^5 cells/mL in a 12-well plate and were transfected with plasmids (an AP fusion protein of TGF-α, Gα proteins, and human GPR35 or mouse GPR35) 16 h later for 24 h using Lipofectamine 2000 (Life Technologies, Carlsbad, CA, USA), according to the manufacturer's instructions. The following day, transfected HEK-293 cells were re-seeded in a 96-well plate, ligands were added at different concentrations, and the plate was incubated for 1 h. Conditioned medium was transferred into another empty 96-well plate and para-nitrophenyl phosphate (p-NPP (N4645, Sigma-Aldrich))-containing solution was added to the conditioned medium plate and to the cell plate. The absorbance of the plate contents was measured for 405 nm, 0 and 1 h after treatment of p-NPP-containing solution. The ratio of the two absorbance values was used as a measure of GPR35 activation (Inoue *et al*., 2012; Park *et al*., 2018).

Statistics

Results are expressed as means ± standard error (SE) of the indicated number of individual values. Statistical significance was determined via analysis of variance (ANOVA) with turkey's post hoc test, and s *p*-values <0.05 were considered statistically significant. Analyses were performed using GraphPad Prism software (GraphPad Software, Inc., La Jolla, CA, USA).

RESULTS

Protective effect of lodoxamide on CCl_4-induced liver fibrosis

Intraperitoneal injection of CCl_4 twice a week for eight weeks was performed to induce liver fibrosis. Lodoxamide and/or CID2745687 were administrated orally every day for the last 4 weeks. Body and liver weights were unchanged after administration of CCl_4, lodoxamide, and CID2745687 (Supplementary Fig. 1A, 1B). The ratio of liver to body weight was also unchanged (Supplementary Fig. 1C). Serum AST and ALT levels were elevated by CCl_4 treatment, implying liver injury, although these levels were unchanged after lodoxamide and CID2745687 treatment (Fig. 1).

In order to measure histological changes induced by chronic liver fibrosis, the liver tissues were stained with H&E (Fig. 2). Compared to normal tissue (control), CCl_4 induced severe in-

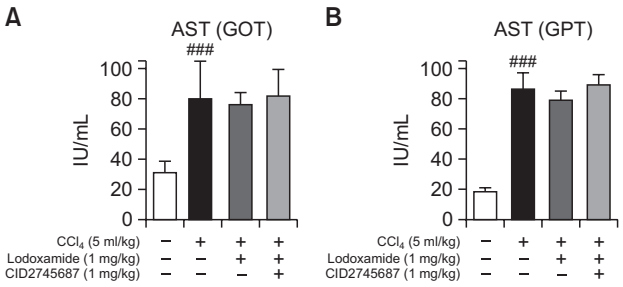

Fig. 1. Changes of aspartate aminotransferase (AST) and alanine aminotransferase (ALT) levels in serum after treatment with CCl_4, lodoxamide, and CID2745687. (A) Serum AST levels after 8-week treatment, (B) serum ALT levels after 8-week treatment. The values shown are means ± SEs (n=5). Statistical significance: $^{###}p$<0.001 vs. vehicle-treated mice.

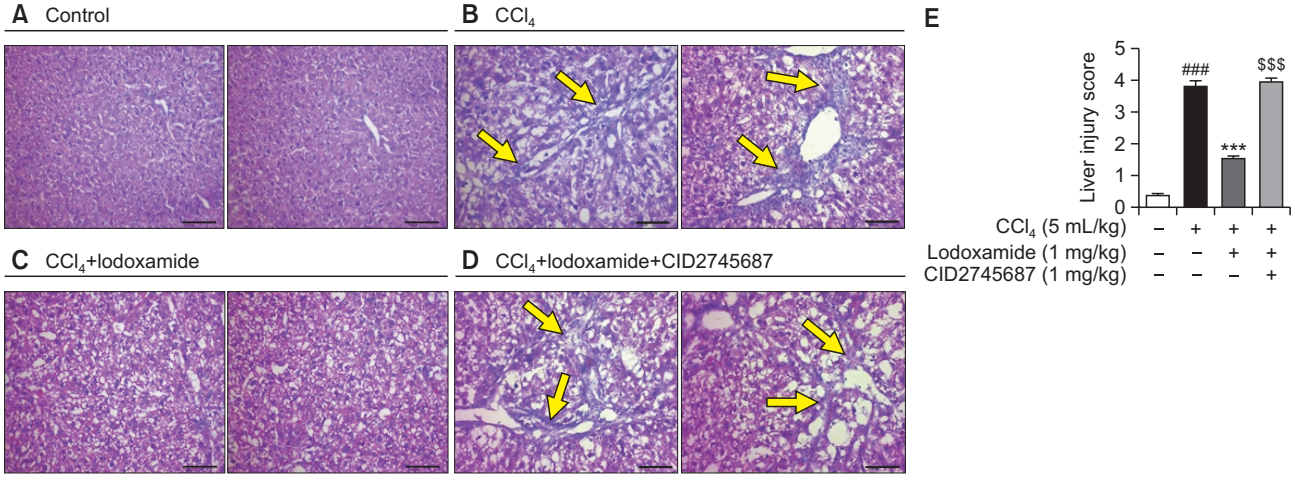

Fig. 2. Histological changes in liver sections after treatment with CCl_4, lodoxamide, and CID2745687. After 8-week treatment, histological analysis was performed using H&E staining in liver sections. Two representative images are provided for each group (n=5). (A) Vehicle-treated mice, (B) CCl_4-treated mice, (C) CCl_4 plus lodoxamide-treated mice, (D) CCl_4 plus lodoxamide and CID2745687-treated mice (scale bar: 100 μm). (E) Liver injury was semi-quantitatively evaluated and shown as histograms. The values shown are means ± SEs (n=5). Statistical significance: $^{###}p$<0.001 vs. vehicle-treated mice, $^{***}p$<0.001 vs. CCl_4-treated mice, and $^{\$\$\$}p$<0.001 vs. CCl_4 plus lodoxamide-treated mice.

jury, which appears as injured areas in the slide. Lodoxamide protected from the CCl_4-induced injury and co-administration of CID2745687 inhibited lodoxamide-mediated protective effects (Fig. 2). Liver injury was semi-quantitatively evaluated using a subjective scale of 0-5, as previously described (Lim *et al*., 2016). Quantitative evaluation of liver injury confirmed the protective effect of lodoxamide and inhibition by CID2745687 (Fig. 2E).

In order to confirm liver fibrosis, Masson's trichrome staining was also performed. As shown in Fig. 3, CCl_4 induced fibrosis, as shown by blue-stained areas, while liver tissues from lodoxamide-treated mice exhibited less fibrosis. CID2745687 inhibited lodoxamide's protective effects (Fig. 3). Degree of liver fibrosis was semi-quantitatively evaluated using a subjective scale of 0-5 in Ishak stage (Lim *et al*., 2016; Nallagangula *et al*., 2017). The result clearly showed the protective effect of lodoxamide and inhibition by CID2745687 (Fig. 3).

Next, changes in the mRNA levels of pro-fibrotic markers

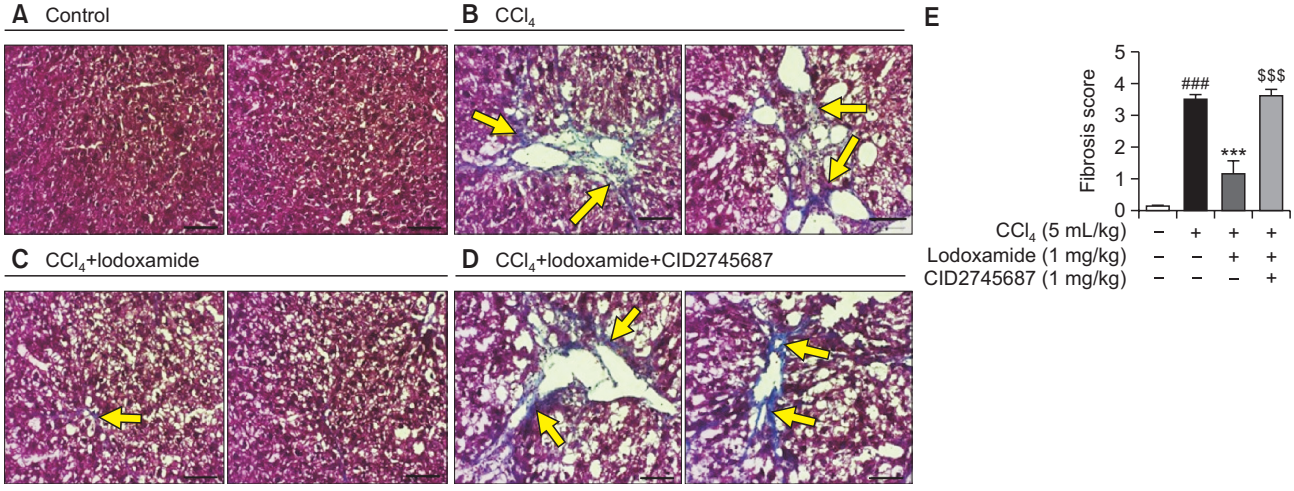

Fig. 3. Fibrotic changes in liver sections after treatment with CCl_4, lodoxamide, and CID2745687. After 8-week treatment, analysis of fibrosis in liver sections was performed using Masson's trichrome staining. Two representative images are provided for each group (n=5). (A) Vehicle-treated mice, (B) CCl_4-treated mice, (C) CCl_4 plus lodoxamide-treated mice, (D) CCl_4 plus lodoxamide and CID2745687-treated mice (scale bar: 100 μm). (E) Liver fibrosis was semi-quantitatively evaluated and shown as histograms. The values shown are means ± SEs (n=5). Statistical significance: $^{###}p$<0.001 vs. vehicle-treated mice, ***p<0.001 vs. CCl_4-treated mice, and $^{\$\$\$}p$<0.001 vs. CCl_4 plus lodoxamide-treated mice.

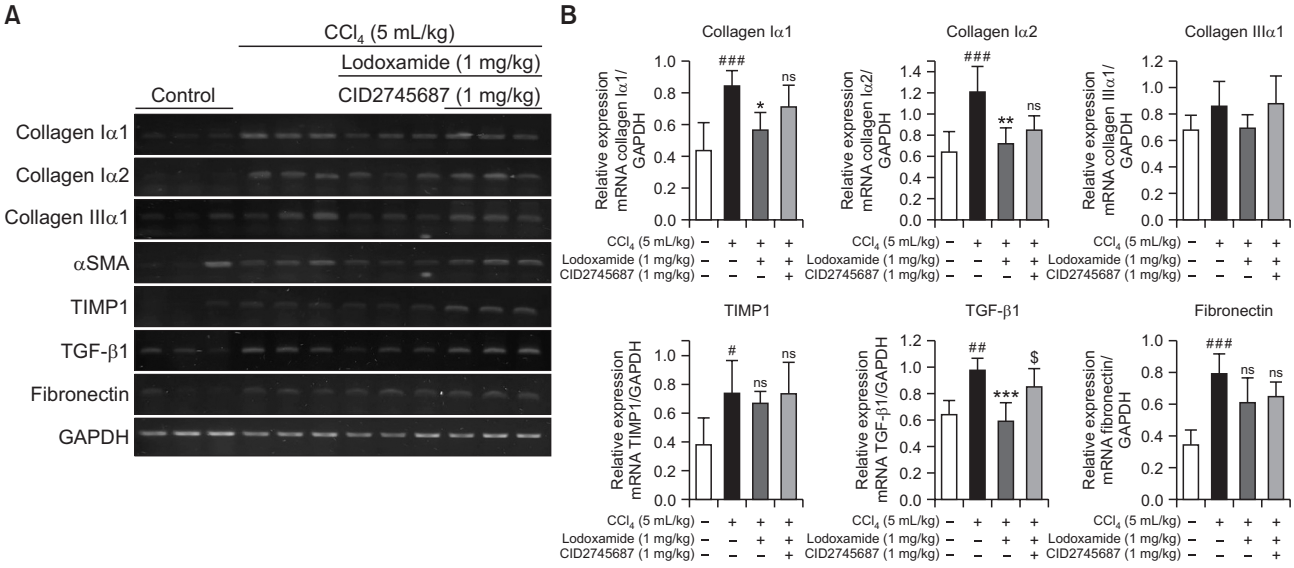

Fig. 4. Changes in mRNA expression of pro-fibrotic cytokines in liver tissues after treatment with CCl_4, lodoxamide, and CID2745687. (A) RT-PCR analysis of the pro-fibrotic proteins collagen Iα1, collagen Iα2, collagen IIIα1, αSMA, TIMP1, TGF-β1, and fibronectin was performed using mRNA isolated from liver tissues after 8-week treatment. (B) mRNA levels are expressed as ratios to GAPDH mRNA levels. The values shown are means ± SEs (n=5). Statistical significance: $^{#}p$<0.05, $^{##}p$<0.01, $^{###}p$<0.001 vs. vehicle-treated mice, *p<0.05, **p<0.01, ***p<0.001 vs. CCl_4-treated mice, and $^{\$}p$<0.05 vs. CCl_4 plus lodoxamide-treated mice.

were measured in liver tissues. mRNA expression of the profibrotic markers, collagen Iα1, collagen Iα2, collagen IIIα1, αSMA, TIMP1, TGF-β1, and fibronectin in CCl_4-treated liver tissues was measured by RT-PCR (Fig. 4A). mRNA levels of collagen Iα1, collagen Iα2, TIMP1, TGF-β1, and fibronectin were significantly elevated in livers of CCl_4-treated mice, and CCl_4-induced increase of collagen Iα1, collagen Iα2, and TGF-β1 was suppressed in lodoxamide-treated mice (Fig. 4B). CID2745687 co-treatment reversed the effects of lodoxamide treatment on TGF-β1 significantly, but not on others. Collagen IIIα1 and αSMA were unchanged by CCl_4 treatment (Fig. 4A).

Lodoxamide activated human GPR35 but not mouse GPR35 in HEK293 cells

Although CID2745687 reversed the lodoxamide-mediated protection against liver injury and fibrosis, it did not reverse the lodoxamide-mediated inhibition on mRNA expression of collagen Iα1 and collagen Iα2. This raised a question on pharmacological characters of lodoxamide, because there has been an issue of species selectivity for many GPR35 agonists, such as zaprinast and pamoic acid (Taniguchi *et al*., 2006; Jenkins *et al*., 2010; Zhao *et al*., 2010; Neetoo-Isseljee *et al*., 2013). Although lodoxamide was reported as a potent agonist of human and rat GPR35, its activity on mouse GPR35 was a question. Therefore, in order to measure the activity of human or mouse GPR35, an AP-TGF-α shedding assay was applied (Inoue *et al*., 2012; Park *et al*., 2018). Human or mouse GPR35 were overexpressed in HEK293 cells and their activities were measured via AP-TGF-α shedding assay. Lodoxamide activated human GPR35 in a concentration-dependent manner (Fig. 5), although in mouse GPR35-transfected cells, AP-TGF-α shedding assay was not observed, which is contrasting to a previous study (MacKenzie *et al*., 2014; Milligan, 2018).

DISCUSSION

The present study reports the first demonstration of the protective effects of lodoxamide on liver fibrosis. Two key findings are reported. First, lodoxamide protected from CCl_4-mediated liver fibrosis in mice and CID2745687 reversed these protective effects. Second, lodoxamide activated human GPR35 but not mouse GPR35 in an AP-TGF-α shedding assay.

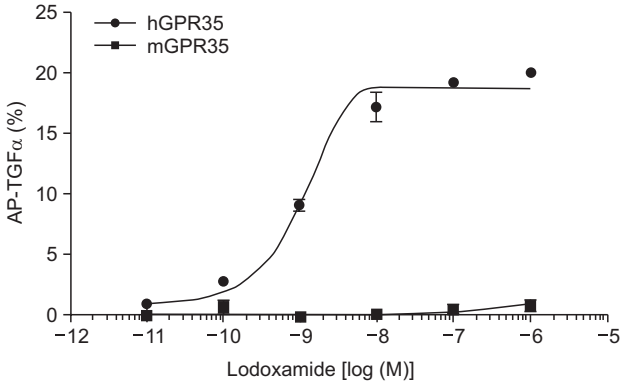

Fig. 5. Lodoxamide induced the activation of human GPR35 but not mouse GPR35. Concentration-response curve of lodoxamide determined via AP-TGFα shedding assay. Lodoxamide was investigated with regard to human or mouse GPR35 co-expressed with a mixture of eight Gα proteins in HEK-293 cells. The values shown are means ± SEs (n=3).

Lodoxamide was used here as a GPR35 agonist, as it was originally reported to be the most potent agonist of human and rat GPR35 (MacKenzie *et al*., 2014). However, in this study, we found that mouse GPR35 was not activated by lodoxamide in an AP-TGF-α shedding assay. This was not reported in the original report (MacKenzie *et al*., 2014). Recently, Milligan (2018) showed lodoxamide-induced activation of mouse GPR35 in β-arrestin-2 recruitment assay at μM concentrations. This is contrasting to no activation of mouse GPR35 by lodoxamide in our AP-TGF-α shedding assay, but the 4000-fold lower potency of lodoxamide in mouse GPR35 compared to those in human and rat GPR35 in β-arrestin-2 recruitment assay supports our observation (Milligan, 2018). Therefore, we unexpectedly faced difficulties in interpreting the *in vivo* efficacy of lodoxamide on liver fibrosis. Similarly, in mouse primary hepatocytes, the half-maximal effective concentration (EC_{50}) of lodoxamide was estimated to be 6.1 nM (Nam *et al*., 2019), which cannot be explained by our observation of that lodoxamide did not activate mouse GPR35 in AP-TGF-α shedding assay. Therefore, the anti-fibrotic effects of lodoxamide and its reverse by CID2745687 in mice were observed. However, in AP-TGF-α shedding assay, specificity of lodoxamide on mouse GPR35 is questioned. Two interpretation are possible. A simple interpretation may be that the *in vivo* effects of lodoxamide might be mediated by target molecules other than GPR35. The other explanation might be that lodoxamide acts on mouse GPR35 *in vivo*, but its action is not reproduced *in vitro* assay systems because an unknown factor endogenously expressed in the liver is not expressed in HEK293 cells such as co-receptors or heterdimers of GPCRs (Smith *et al*., 2017; Borroto-Escuela *et al*., 2018).

CID2745687 was reported as a potent and effective antagonist on human GPR35 but not of rodent GPR35 orthologs (Jenkins *et al*., 2012). However, in other reports CID274568 was reported to inhibit agonist-induced activation of mouse GPR35 in HEK293 cells, mouse astrocytes, and mouse colon epithelial cells (Zhao *et al*., 2010; Berlinguer-Palmini *et al*., 2013; Tsukahara *et al*., 2017). Although inhibitory effect of CID2745687 on lodoxamide action was observed in mice. we cannot exclude the possibility of off-target effects of CID2745687. This may suggest that lodoxamide and CID2745687 act as an agonist and an antagonist, respectively, of the same unknown target in mice. In our previous study on hepatocytes, CID2745687 reversed the effects of lodoxamide when administrated at a dose of 10 times greater (10 mg/kg) than that of lodoxamide (1 mg/kg) *in vivo* (Nam *et al*., 2019). However, in the present study, the same dose of CID2745687 effectively reversed the effects of lodoxamide, suggesting different affinities between the two experimental models of hepatic steatosis and hepatic fibrosis. Further investigation is necessary to elucidate the different efficacies of CID2745687.

In summary, lodoxamide attenuates CCl_4-induced liver fibrosis in mice and CID2745687 reverses the lodoxamide's effect. However, involvement of mouse GPR35 in the effects is questioned in AP-TGF-α shedding assay. Therefore, we reported the results to accelerate drug development for liver fibrosis and raise concerns how lodoxamide protects against liver fibrosis *in vivo* and whether GPR35 is involved in the action.

CONFLICT OF INTEREST

Authors declare there is no conflict of interest.

ACKNOWLEDGMENTS

This study was supported by a 2-year research grant from Pusan National University.

REFERENCES

Bataller, R. and Brenner, D. A. (2005) Liver fibrosis. *J. Clin. Invest.* **115**, 209-218.

Berlinguer-Palmini, R., Masi, A., Narducci, R., Cavone, L., Maratea, D., Cozzi, A., Sili, M., Moroni, F. and Mannaioni, G. (2013) GPR35 activation reduces Ca^{2+} transients and contributes to the kynurenic acid-dependent reduction of synaptic activity at CA3-CA1 synapses. *PLoS ONE* **8**, e82180.

Borroto-Escuela, D. O., Rodriguez, D., Romero-Fernandez, W., Kapla, J., Jaiteh, M., Ranganathan, A., Lazarova, T., Fuxe, K. and Carlsson, J. (2018) Mapping the interface of a GPCR dimer: a structural model of the A2A adenosine and D2 dopamine receptor heteromer. *Front. Pharmacol.* **9**, 829.

Choi, J. S., Kim, J. K., Yang, Y. J., Kim, Y., Kim, P., Park, S. G., Cho, E. Y., Lee, D. H. and Choi, J. W. (2015) Identification of cromolyn sodium as an anti-fibrotic agent targeting both hepatocytes and hepatic stellate cells. *Pharmacol. Res.* **102**, 176-183.

Fallarini, S., Magliulo, L., Paoletti, T., de Lalla, C. and Lombardi, G. (2010) Expression of functional GPR35 in human iNKT cells. *Biochem. Biophys. Res. Commun.* **398**, 420-425.

Funke, M., Thimm, D., Schiedel, A. C. and Muller, C. E. (2013) 8-Benzamidochromen-4-one-2-carboxylic acids: potent and selective agonists for the orphan G protein-coupled receptor GPR35. *J. Med. Chem.* **56**, 5182-5197.

Heynen-Genel, S., Dahl, R., Shi, S., Sauer, M., Hariharan, S., Sergienko, E., Dad, S., Chung, T. D. Y., Stonich, D., Su, Y., Caron, M., Zhao, P., Abood, M. E. and Barak, L. S. (2010a) Selective GPR35 antagonists - probes 1 & 2. In Probe Reports from the NIH Molecular Libraries Program. Bethesda (MD).

Heynen-Genel, S., Dahl, R., Shi, S., Sauer, M., Hariharan, S., Sergienko, E., Dad, S., Chung, T. D. Y., Stonich, D., Su, Y., Zhao, P., Caron, M. G., Abood, M. E. and Barak, L. S. (2010b) Selective GPR35 Antagonists - Probe 3. In Probe Reports from the NIH Molecular Libraries Program, Bethesda (MD).

Inoue, A., Ishiguro, J., Kitamura, H., Arima, N., Okutani, M., Shuto, A., Higashiyama, S., Ohwada, T., Arai, H., Makide, K. and Aoki, J. (2012) TGFa shedding assay: an accurate and versatile method for detecting GPCR activation. *Nat. Methods* **9**, 1021-1029.

Jenkins, L., Brea, J., Smith, N. J., Hudson, B. D., Reilly, G., Bryant, N. J., Castro, M., Loza, M. I. and Milligan, G. (2010) Identification of novel species-selective agonists of the G-protein-coupled receptor GPR35 that promote recruitment of b-arrestin-2 and activate Ga13. *Biochem. J.* **432**, 451-459.

Jenkins, L., Harries, N., Lappin, J. E., MacKenzie, A. E., Neetoo-Isseljee, Z., Southern, C., McIver, E. G., Nicklin, S. A., Taylor, D. L. and Milligan, G. (2012) Antagonists of GPR35 display high species ortholog selectivity and varying modes of action. *J. Pharmacol. Exp. Ther.* **343**, 683-695.

Lim, S. W., Lee, D. R., Choi, B. K., Kim, H. S., Yang, S. H., Suh, J. W. and Kim, K. S. (2016) Protective effects of a polymethoxy flavonoids-rich *Citrus aurantium* peel extract on liver fibrosis induced by bile duct ligation in mice. *Asian Pac. J. Trop. Med.* **9**, 1158-1164.

MacKenzie, A. E., Caltabiano, G., Kent, T. C., Jenkins, L., McCallum, J. E., Hudson, B. D., Nicklin, S. A., Fawcett, L., Markwick, R., Charlton, S. J. and Milligan, G. (2014) The antiallergic mast cell stabilizers lodoxamide and bufrolin as the first high and equipotent agonists of human and rat GPR35. *Mol. Pharmacol.* **85**, 91-104.

Milligan, G. (2018) G protein-coupled receptors not currently in the spotlight: free fatty acid receptor 2 and GPR35. *Br. J. Pharmacology* **175**, 2543-2553.

Nallagangula, K. S., Nagaraj, S. K., Venkataswamy, L. and Chandrappa, M. (2017) Liver fibrosis: a compilation on the biomarkers status and their significance during disease progression. *Future Sci. OA* **4**, FSO250.

Nam, S. Y., Park, S. J. and Im, D. S. (2019) Protective effect of lodoxamide on hepatic steatosis through GPR35. *Cell Signal.* **53**, 190-200.

Neetoo-Isseljee, Z., MacKenzie, A. E., Southern, C., Jerman, J., McIver, E. G., Harries, N., Taylor, D. L. and Milligan, G. (2013) High-throughput identification and characterization of novel, species-selective GPR35 agonists. *J. Pharmacol. Exp. Ther.* **344**, 568-578.

O'Dowd, B. F., Nguyen, T., Marchese, A., Cheng, R., Lynch, K. R., Heng, H. H., Kolakowski, L. F., Jr. and George, S. R. (1998) Discovery of three novel G-protein-coupled receptor genes. *Genomics* **47**, 310-313.

Park, S. J. and Im, D. S. (2019) Deficiency of sphingosine-1-phosphate receptor 2 ($S1P_2$) attenuates bleomycin-induced pulmonary fibrosis. *Biomol. Ther. (Seoul)* **27**, 318-326.

Park, S. J., Lee, S. J., Nam, S. Y. and Im, D. S. (2018) GPR35 mediates lodoxamide-induced migration inhibitory response but not CXCL17-induced migration stimulatory response in THP-1 cells; is GPR35 a receptor for CXCL17? *Br. J. Pharmacol.* **175**, 154-161.

Smith, T. H., Li, J. G., Dores, M. R. and Trejo, J. (2017) Protease-activated receptor-4 and purinergic receptor P2Y12 dimerize, co-internalize, and activate Akt signaling via endosomal recruitment of β-arrestin. *J. Biol. Chem.* **292**, 13867-13878.

Taniguchi, Y., Tonai-Kachi, H. and Shinjo, K. (2006) Zaprinast, a well-known cyclic guanosine monophosphate-specific phosphodiesterase inhibitor, is an agonist for GPR35. *FEBS Lett.* **580**, 5003-5008.

Thimm, D., Funke, M., Meyer, A. and Muller, C. E. (2013) 6-Bromo-8-(4-[(3)H]methoxybenzamido)-4-oxo-4H-chromene-2-carboxylic acid: a powerful tool for studying orphan G protein-coupled receptor GPR35. *J. Med. Chem.* **56**, 7084-7099.

Tsukahara, T., Hamouda, N., Utsumi, D., Matsumoto, K., Amagase, K. and Kato, S. (2017) G protein-coupled receptor 35 contributes to mucosal repair in mice via migration of colonicepithelial cells. *Pharmacol. Res.* **123**, 27-39.

Wang, J., Simonavicius, N., Wu, X., Swaminath, G., Reagan, J., Tian, H. and Ling, L. (2006) Kynurenic acid as a ligand for orphan G protein-coupled receptor GPR35. *J. Biol. Chem.* **281**, 22021-22028.

Yang, Y., Lu, J. Y., Wu, X., Summer, S., Whoriskey, J., Saris, C. and Reagan, J. D. (2010) G-protein-coupled receptor 35 is a target of the asthma drugs cromolyn disodium and nedocromil sodium. *Pharmacology* **86**, 1-5.

Zhao, P., Sharir, H., Kapur, A., Cowan, A., Geller, E. B., Adler, M. W., Seltzman, H. H., Reggio, P. H., Heynen-Genel, S., Sauer, M., Chung, T. D., Bai, Y., Chen, W., Caron, M. G., Barak, L. S. and Abood, M. E. (2010) Targeting of the orphan receptor GPR35 by pamoic acid: a potent activator of extracellular signal-regulated kinase and b-arrestin2 with antinociceptive activity. *Mol. Pharmacol.* **78**, 560-568.